Available online at www.sciencedirect.com

ScienceDirect

Polymer 49 (2008) 1211–1219

polymer

www.elsevier.com/locate/polymer

Synthesis and properties of novel electrophosphorescent conjugated polyfluorenes based on aminoalkyl-fluorene and bipyridine with rhenium(I) complexes

Yong Zhang, Zhe Huang, Wenjin Zeng, Yong Cao*

Institute of Polymer Optoelectronic Materials and Devices, Key Laboratory of Special Functional Materials of the Ministry of Education, South China University of Technology, Guangzhou 510640, China

Received 8 November 2007; received in revised form 26 December 2007; accepted 14 January 2008
Available online 26 January 2008

Abstract

Novel bipyridine-based aminoalkyl-polyfluorene and their corresponding rhenium complex-contained copolymers with different rhenium complex contents in polymer backbone were synthesized by Suzuki polymerization and post-polymerization, respectively. The aminoalkyl-polyfluorenes have good solubility in organic solvents and also are able to dissolve in methanol by adding a few drops of acetic acid. The solubility in polar solvents such as alcohol provides a great advantage in fabrication of multi-layer PLEDs. However, the rhenium complex-based copolymers become insoluble in common organic solvents; instead have a good solubility in polar solvents, such as methanol and DMF. The optoelectronic and electroluminescent properties of these copolymers (bipyridine- and rhenium-based copolymers) were investigated. The electroluminescent properties of these copolymers were found to have similar device performances by using high work function metal (Al) and low work function metal (Ba) as cathodes. We also found that these rhenium copolymers can be used as the electron transport layer in PLED. After inserting a thin rhenium copolymer layer between emission layer (P-PPV or PFO-DBT15) and cathode, a great improvement in EL performance could be achieved.

Keywords: Polyfluorene; Bipyridine; Rhenium complex

1. Introduction

Conjugated polymeric light-emitting materials have attracted considerable attention since the first report of electroluminescence in poly(*p*-phenylenevinylene) [1]. Conjugated polymers provide many advantages over traditional organic small molecular light-emitting materials in device processing, such as easy fabrication in large area devices and good mechanical properties [2–6]. In the past decades, varieties of conjugated polymers, such as poly(*p*-phenylenevinylene)s (PPVs), poly(*p*-phenyleneethynylene)s (PPEs), poly(*p*-phenylene)s (PPPs) and polyfluorenes (PFs), have been investigated as light-emitting materials [2–6]. Recently, it has been shown that the conjugated polymers with aminoalkyl-substituted fluorene in the polymer backbones (PFN) and the corresponding cationic polyelectrolyte can be used as emitting layer with high work function metals such as Au, Ag and Al as cathodes and the device efficiency of which is comparable with that by using low work function metals such as Ca and Ba [7–12]. The emission color of such devices can be tuned from green to red and near-IR by incorporating varieties of narrow-band gap co-monomers such as 2,1,3-benzothiazole [8], 4,7-dithiophen-2′-yl-2,1,3-benzothiazole [9], iridium complex [10–12], into the polymer main chain. Importantly, this kind of aminoalkyl-polyfluorenes could also be used as electron injection layer coated on top of conventional emitting polymers and good device performance was achieved with such PFN/Al bilayer cathode [13,14].

Recently, electrophosphorescent polymer light-emitting diodes (PLEDs) based on metal complexes, such as iridium, ruthenium and rhenium complexes, have received a great attention and widely been investigated due to their high

---

* Corresponding author. Tel.: +86 20 87114609; fax: +86 20 87110606.
E-mail address: poycao@scut.edu.cn (Y. Cao).

0032-3861/$ - see front matter © 2008 Elsevier Ltd. All rights reserved.
doi:10.1016/j.polymer.2008.01.042

emission efficiency by fully utilizing singlet and triplet excitons. The chemistry and photophysical properties of chlorotricarbonyl rhenium complexes have been studied extensively due to their potential applications as light-emitting materials, photocatalysts, photosensitizers and in solar energy conversion [15–20]. Emission of rhenium complexes is usually assigned to the long lived metal-to-ligand charge transfer (^{3}MLCT) excited state transitions although emission from intraligand (^{3}IL) states was also reported. Rhenium complexes also have been incorporated into PPV and PPE backbone [18,19,21]. Recently, Ma et al. have reported PFs incorporated with *fac*-(Bpy)Re(I)$(CO)_3Cl$ chromophores in the backbones, although no detailed device performances were reported [22].

In this paper, we synthesized a new series of aminoalkyl-substituted polyfluorene copolymerized with an electron-accepted monomer 2,2′-bipyridine by palladium-catalyzed Suzuki cross-coupling reaction. The trichlorotricarbonyl rhenium complexes were incorporated into the backbones of the copolymers through a highly active replacement reaction of 2,2′-bipyridine element by post-condensation treatment. Photo-/electroluminescent properties of the resulting copolymers are investigated and discussed. The device results using the rhenium complex-based copolymers as electron injection layer are also reported.

2. Experimental section

2.1. General details

All manipulations involving air-sensitive reagents were performed under an atmosphere of dry argon. All reagents, unless otherwise specified, were obtained from Aldrich, Acros and TCI Chemical Co. and used as-received. All the solvents used were further purified before use. The ^{1}H and ^{13}C NMR spectra were collected on a Bruker DRX 300 spectrometer operating, respectively, at 300 and 75 MHz. Number-average (M_n) and weight-average (M_w) molecular weights were determined by a Waters GPC 2410 in tetrahydrofuran (THF) using a calibration curve of polystyrene standards. Elemental analyses were performed on Vario EL Elemental Analysis Instrument (Elementar Co.). UV–vis absorption spectra were recorded on an HP 8453 UV–vis spectrophotometer. PL spectra were recorded on Instaspec IV CCD spectrophotometer (Oriel Co.). Cyclic voltammetry was carried out on a CHI660A electrochemical workstation in a solution of tetrabutylammonium hexafluorophosphate (Bu_4NPF_6) (0.1 M) in acetonitrile at a scan rate of 50 mV/s at room temperature under the protection of argon. A platinum electrode was coated with a thin polymer film and was used as the working electrode. A Pt wire was used as the counter electrode and a saturated calomel electrode (SCE) was used as the reference electrode. FT-IR spectra were recorded on a Bruker spectrophotometer in the 400–4000 cm^{-1} region, using a thin film drop-coated on a KBr plate.

The PLEDs were fabricated on indium tin oxide (ITO) covered glass substrates. Polymers were dissolved in toluene (for PFN–Bpy copolymers) or methanol (for rhenium copolymers) and filtered through a 0.45 μm filter. Poly(3,4-ethylenedioxythiophene) (PEDOT) doped with poly(styrene-sulfonic acid) (PSS) (Baytron-P 4083, Bayer AG) or polyvinylcarbazole (PVK, Aldrich) from 1,1,2,2-tetrachloroethane solution was spin-coated onto the ITO substrate followed by drying in a vacuum oven at 80 °C for 8 h and evacuation at room temperature for PEDOT and PVK coating, respectively. The thickness of PEDOT and PVK layers was at around 150 nm. Polymers of this study as an active layer were spin-coated on top of PEDOT or PVK layer followed by deposition of 200 nm Al (or 4 nm Ba and 200 nm Al) as a cathode under a vacuum of 1×10^{-4} Pa. The polymer film thickness of the active layers was at around 70 nm, as measured with an Alfa step 500 Surface Profiler (Tencor). Current–voltage (I–V) characteristics were recorded with a Keithley 236 source meter. EL spectra were recorded by Oriel Instaspec IV CCD Spectrograph. Luminance and external quantum efficiencies were determined by using a photodiode calibrated by a PR-705 SpectraScan Spectrophotometer (Photo Research) and integrating sphere (model IS 080, Labspere), respectively.

2.2. Materials

Compounds 5,5′-dibromo-2,2′-bipyridine (**2**) [23], 2,7-bis-(4,4,5,5-tetramethyl-1,3,2-dioxaborolan-2-yl)-9,9-dioctylfluorene (**3**) [24–26] and 2,7-dibromo-9,9-bis(3′-(*N*,*N*-dimethylamino)-propyl)fluorene (**4**) [7] were prepared according to the published procedures.

2.3. Synthesis of polymers: PFN–Bpy05

The preparation of polymer PFN–Bpy05 is given as a typical example. 2,7-Bis(4,4,5,5-tetramethyl-1,3,2-dioxaborolan-2-yl)-9,9-dioctylfluorene (**3**) (642 mg, 1.00 mmol), 2,7-dibromo-9,9-bis(3′-(*N*,*N*-dimethylamino)propyl)fluorene (**4**) (489 mg, 0.99 mmol), 5,5′-dibromo-2,2′-bipyridine (**2**) (3.14 mg, 0.01 mmol), tetrakis (triphenyl phosphine) palladium [$(PPh_3)_4Pd(0)$] (10 mg), and several drops Aliquat 336 were dissolved in a mixture of 8 mL toluene and 4 mL 2 M Na_2CO_3 aqueous solution. The mixture was refluxed with vigorous stirring for 2 days under argon atmosphere. After the mixture was cooled to room temperature, the solution was filtered and the filtrate was poured into methanol. The precipitated material was recovered by filtration through a funnel. The resulted solid material was washed for 24 h using acetone to remove oligomers and catalyst residues (0.59 g, yield: 81%). ^{1}H NMR ($CDCl_3$): $\delta = 7.87$–7.84, 7.73–7.62, 2.19–2.08, 1.75, 1.15, 0.86–0.81. ^{13}C NMR ($CDCl_3$): $\delta = 151.80$, 151.21, 140.70, 140.43, 140.09, 126.43, 126.14, 121.44, 120.04, 59.80, 55.38, 55.07, 45.33, 31.80, 30.11, 29.28, 22.61, 14.09. Element Anal. Found: C, 85.32%; H, 9.53%; N, 3.46%. $M_n = 16\,701$, $M_w = 37\,400$, PDI = 2.24.

2.4. PFN–Bpy5

Monomer feed ratio: 2,7-bis(4,4,5,5-tetramethyl-1,3,2-dioxaborolan-2-yl)-9,9-dioctylfluorene (**3**) (1 mmol), 2,7-dibromo-9,9-bis(3′-(*N*,*N*-dimethylamino)propyl)fluorene (**4**)

(0.9 mmol), 5,5′-dibromo-2,2′-bipyridine (**2**) (0.1 mmol, yield: 71%). ^{1}H NMR ($CDCl_3$): $\delta = 9.09$, 8.60, 8.16, 7.87–7.84, 7.73–7.67, 2.19–2.08, 1.77, 1.15, 0.86–0.81. ^{13}C NMR ($CDCl_3$): $\delta = 151.80$, 151.19, 140.71, 140.06, 126.45, 126.13, 121.43, 120.09, 59.79, 55.39, 55.06, 45.31, 31.80, 30.12, 29.28, 22.61, 14.09. Element Anal. Found: C, 87.01%; H, 9.43%; N, 3.71%. $M_n = 24\,317$, $M_w = 55\,950$, PDI = 2.30.

2.5. PFN–Bpy10

Monomer feed ratio: 2,7-bis(4,4,5,5-tetramethyl-1,3,2-dioxaborolan-2-yl)-9,9-dioctylfluorene (**3**) (1 mmol), 2,7-dibromo-9,9-bis(3′-(*N*,*N*-dimethylamino)propyl)fluorene (**4**) (0.8 mmol), 5,5′-dibromo-2,2′-bipyridine (**2**) (0.2 mmol) (yield: 76%). ^{1}H NMR ($CDCl_3$): $\delta = 9.08$, 8.63–8.60, 8.19–8.16, 7.87–7.84, 7.73–7.67, 2.19–2.08, 1.71, 1.15, 0.86–0.81. ^{13}C NMR ($CDCl_3$): $\delta = 151.80$, 151.20, 147.86, 140.71, 140.43, 140.06, 135.14, 128.79, 127.21, 126.44, 126.11, 121.45, 120.94, 120.06, 59.78, 55.39, 55.07, 45.31, 31.80, 30.11, 29.28, 29.25, 22.61, 14.09. Element Anal. Found: C, 86.34%; H, 9.83%; N, 4.11%. $M_n = 19\,275$, $M_w = 54\,710$, PDI = 2.84.

2.6. PFN–Bpy20

Monomer feed ratio: 2,7-bis(4,4,5,5-tetramethyl-1,3,2-dioxaborolan-2-yl)-9,9-dioctylfluorene (**3**) (1 mmol), 2,7-dibromo-9,9-bis(3′-(*N*,*N*-dimethylamino)propyl)fluorene (**4**) (0.6 mmol), 5,5′-dibromo-2,2′-bipyridine (**2**) (0.4 mmol) (yield: 68%). ^{1}H NMR ($CDCl_3$): $\delta = 9.08$, 8.63–8.61, 8.20–8.16, 7.87–7.84, 7.74–7.67, 2.19–2.08, 1.71, 1.15, 0.86–0.81. ^{13}C NMR (CDCl3): $\delta = 151.80$, 151.20, 147.86, 140.71, 140.43, 140.06, 135.14, 128.79, 127.21, 126.44, 126.11, 121.45, 120.94, 120.09, 59.78, 55.39, 55.08, 45.31, 31.80, 30.12, 29.28, 29.25, 22.61, 14.09. Element Anal. Found: C, 86.93%; H, 9.27%; N, 4.29%. $M_n = 21\ 350$, $M_w = 36\ 590$, PDI = 1.72.

2.7. Polymer complex with rhenium(I), PFN–BpyRe

The preparation of polymer PFN–Bpy05Re is given as a typical example.

In a 100 mL flask with a magnetic stirring bar was charged PFN–Bpy05 (50 mg) dissolved in 60 mL of toluene. To the polymer solution was added excess pentacarbonylrhenium chloride (25 mg) and the solution was refluxed for 6 h. After the solvent was removed, the yellow solid was washed with toluene and dissolved in methanol and filtered. The yellow-green solid PFN–Bpy05Re was obtained by removing the solvent and dried in vacuum.

PFN–Bpy05Re: FT-IR (cm^{-1}): 480, 509, 661, 754, 812, 887, 911, 1252, 1458, 1614, 1642, 1907, 2024, 2854, 2924, 3425.

PFN–Bpy5Re: FT-IR (cm^{-1}): 478, 508, 553, 661, 751, 814, 886, 910, 1000, 1164, 1251, 1404, 1458, 1609, 1902, 2023, 2856, 2926, 3425.

PFN–Bpy10Re: FT-IR (cm^{-1}): 480, 507, 663, 814, 886, 913, 1251, 1458, 1614, 1908, 2026, 2854, 2927, 3424.

3. Results and discussion

3.1. Synthesis and characterization

The general synthetic routes toward the monomer and copolymers and corresponding rhenium complexes are shown in Schemes 1 and 2. The monomers 5,5′-dibromo-2,2′-bipyridine (**2**), 2,7-bis(4,4,5,5-tetramethyl-1,3,2-dioxaborolan-2-yl)-9,9-dioctylfluorene (**3**) and 2,7-dibromo-9,9-bis(3′-(*N*,*N*-dimethylamino)propyl)fluorene (**4**) were synthesized by following the literature [7,23–26]. The conjugated copolymers were prepared from **2**–**4** by palladium(0)-catalyzed Suzuki cross-coupling reaction. The feed ratios of monomer **2** in copolymers were 0.5, 5, 10 and 20 mol% and these corresponding copolymers were named as PFN–Bpy05, PFN–Bpy5, PFN–Bpy10 and PFN–Bpy20, respectively. All the copolymers are soluble in common organic solvents such as chloroform, toluene, xylene and THF, but insoluble in DMSO and water. However, these copolymers have a good solubility in polar solvent, such as methanol, by adding a trace of weak organic acid, such as acetic acid, due to the weak interaction formed between the nitrogen atoms in copolymer side chains and acetic acid. The M_n values of the copolymers are around $(1.6–2.5) \times 10^4$ Da with a polydispersity index (M_w/M_n) from 1.7 to 2.8. These copolymers were characterized by NMR spectrum and elemental analysis. The chemical shifts in 9.08, 8.63 and 8.19 ppm were ascribed to the protons of bipyridine and the intensity increased with increasing the feed ratio of monomer **2** in the copolymers except for PFN–Bpy05 which has only 1% bipyridine unit. The actual bipyridine molar ratios in PFN–Bpy5, PFN–Bpy10 and PFN–Bpy20 calculated from the ratio of protons in bipyridine and fluorene units in ^{1}H NMR spectra of these copolymers are about 3.5, 9.4 and 18.3%, respectively. It is similar with the feed ratio of monomer **2**.

The rhenium copolymers were prepared by the PFN–Bpy copolymers with excess $Re(CO)_5Cl$ in toluene under reflux (Scheme 2) [22]. The resulted copolymers were precipitated from a clear solution after ~30 min. The corresponding copolymers were named as PFN–Bpy05Re, PFN–Bpy5Re, PFN–Bpy10Re and PFN–Bpy20Re. The copolymers PFN–Bpy05Re, PFN–Bpy5Re and PFN–Bpy10Re are insoluble in toluene, but soluble in CH_3OH, DMSO and DMF. The PFN–Bpy20Re are insoluble in toluene, methanol, but soluble in DMSO and DMF. This is different from the one reported by Ma et al. [22] in which their polymers are soluble in non-polar organic solvents such as toluene. Based on these results, we tentatively speculate that the interaction between aminoalkyl groups and rhenium complex leads to the solubility of rhenium copolymers in polar solvent. The solubility of PFN–BpyRe copolymer in polar solvent such as methanol also is important for fabrication of multi-layer device when this kind of polymer is spin-coated on top of emitting layer avoiding the intermixing between emission layer and transport layer.

Fig. 1 shows the FT-IR spectra of PFN–Bpy05 and PFN–Bpy05Re as an example to discuss the successful incorporation of rhenium complex into copolymer main chain. In the

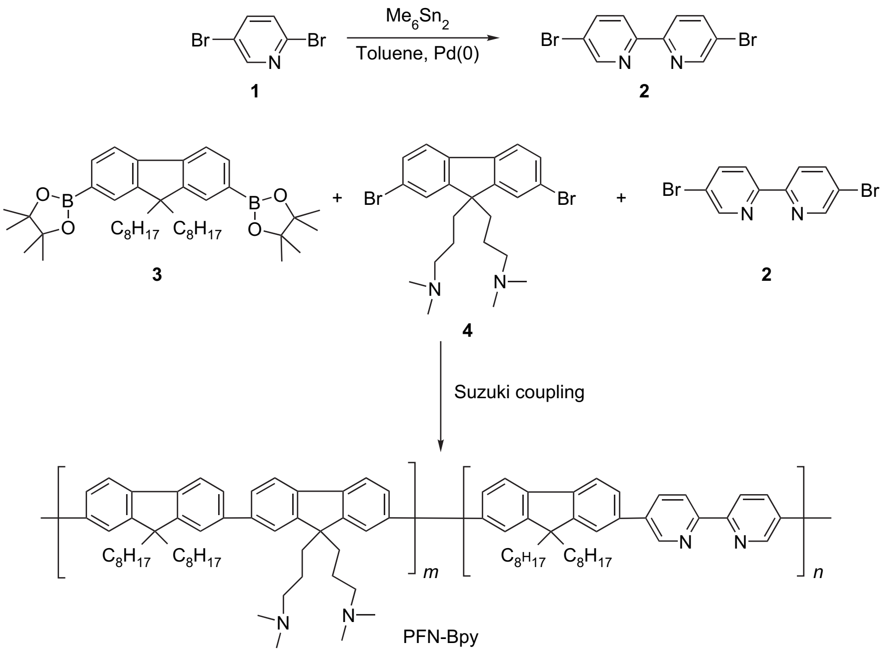

Scheme 1. Synthetic procedure of the copolymers.

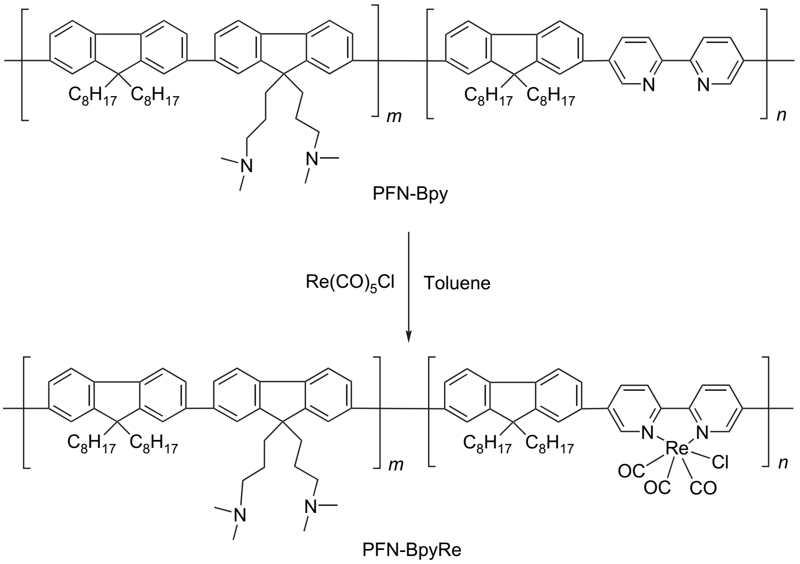

Scheme 2. Synthetic procedure of the rhenium copolymers.

region of 1900–2100 cm^{-1} which is the characteristic feature of carbonyl groups, two new strong vibration peaks at 1907, 2024 cm^{-1} appeared (Fig. 1). These two peaks can be attributed to the carbonyl groups in the rhenium complex of copolymer main chain. In addition, the intensity of these two peaks increased with the increased rhenium complex content in copolymer main chains. Another change in FT-IR spectra of these rhenium copolymers is the C=N vibration peak, which has ~13 cm^{-1} shift toward low wavenumber side after coordinating rhenium complex to bipyridine unit in copolymer main chain as shown in Fig. 1. These results proved that the rhenium complexes had been incorporated into the main chain of the copolymers *via* coordinating with bipyridine.

3.2. Optical and electrochemical properties

The UV–vis absorption and photoluminescence (PL) spectra of the PFN–Bpy copolymers and the rhenium copolymers (PFN–BpyRe) in solution and thin solid film are shown in Figs. 2 and 3. For the PFN–Bpy copolymers (Fig. 2a, PFN–Bpy5 as an example), all PFN–Bpy copolymers show similar absorption spectra in THF, chloroform and CH_3OH (adding a few drops of acetic acid). All these copolymers show absorption maxima at around 390 nm, which could be attributed to the π–π* transition of polyfluorene backbone in THF, chloroform and methanol. The absorption spectra of all polymers are very similar to that of PFN (392 nm) due to no

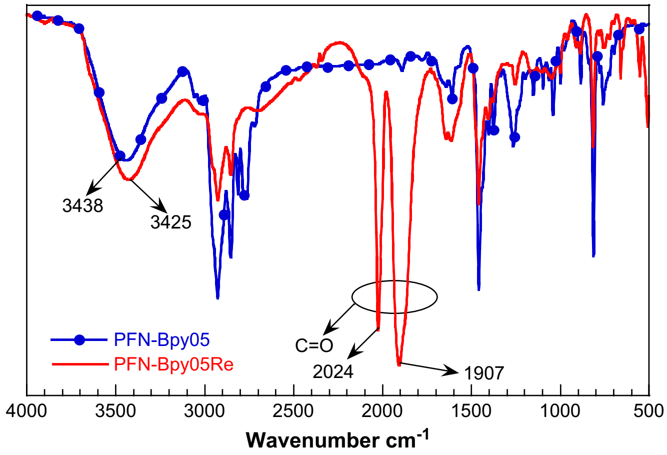

Fig. 1. The FT-IR spectrum of PFN–Bpy05 and PFN–Bpy05Re.

contribution from the bipyridine (low Bpy content in the copolymer) unit in 300–400 nm of the absorption spectra [7]. The UV–vis absorption spectra of the films of the PFN–Bpy copolymers are shown in Fig. 2b. All these polymers show absorptions with a peak at ∼387 nm. Similar to that in the solution, there is only a slight change in the absorption of the polymers compared to that of PFN. Fig. 2a shows the PL spectra of PFN–Bpy5 in solutions. The PL spectra show a typical polyfluorene blue emission, which peaked at around 418, 418 and 416 nm with a shoulder of 440–450 nm in THF, chloroform and methanol, respectively. As seen from Fig. 2b, the PL spectra of PFN–Bpy in solid films also emit blue light and peak at around 421 nm with a shoulder of 477 nm. In addition, there is a weak peak at around 530 nm, the intensity of which increases with increasing the Bpy content. This peak can be attributed to the excimer emission of polymers.

Fig. 3 shows the UV–vis and PL spectra of rhenium copolymers PFN–BpyRe. As seen from Fig. 3a, the absorption spectra of the rhenium copolymers in solid films have a long wavelength absorption band peaking at ∼450 nm, which can be attributed to the rhenium complex unit incorporated into the PFN main chain, the intensity of which increases with increasing the rhenium complex content. As shown in Fig. 3b, in contrast with that of PFN–Bpy the PL spectra of PFN–BpyRe in solid films dominated by a new peak at red region while PFN–Bpy emission was completely quenched. The peak is attributed to the phosphorescent emission from the rhenium complex which peaks at 618 nm and indicates that the energy transfer from PFN segments to the rhenium complex is highly

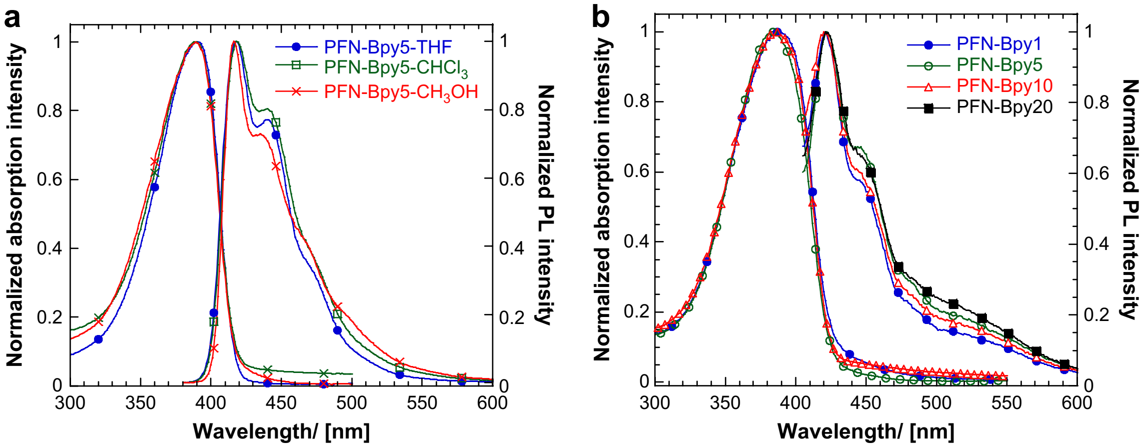

Fig. 2. The UV–vis and PL spectra of PFN–Bpy in solutions (PFN–Bpy5 as an example, (a)) and in solid films (b).

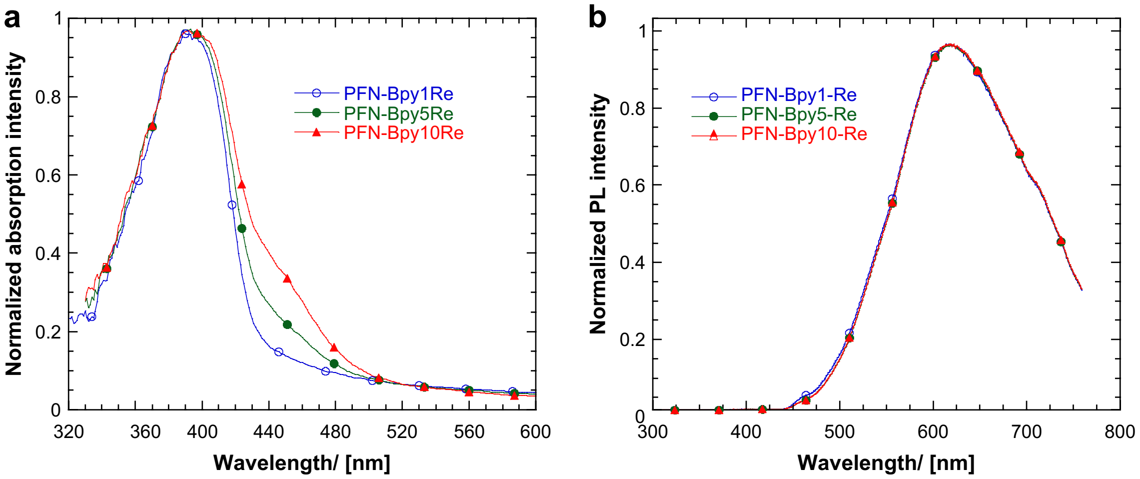

Fig. 3. The UV–vis (a) and PL (b) spectra of PFN–BpyRe in solid film.

efficient. The results also show that the rhenium complex has been successfully incorporated into the copolymer main chain.

The electrochemical behavior of the copolymers was investigated by cyclic voltammetry (CV). Fig. 4 shows the CV curves of PFN–Bpy copolymers, which have the similar electrochemical properties as PFN that contains no bipyridine units [7]. The PFN–Bpy copolymers show a reversible oxidation wave with onset at around 1.20–1.30 V which can be assigned to the oxidation potential of aminoalkyl-substituted copolymer main chains [27]. The oxidation potential of PFN–Bpy is slightly higher than that of PFN due to the incorporating bipyridine units. The reduction peak occurred at around −1.90 to −2.10 V which is very consistent with a reduction wave observed for polyfluorene homocopolymer and copolymers. Table 1 summarizes the oxidation and reduction potentials corresponding to the copolymer main chain. HOMO and LUMO levels of the copolymers are calculated according to empirical formulas $E_{\mathrm{HOMO}} = -e(E_{\mathrm{ox}} + 4.4)$ eV and $E_{\mathrm{LUMO}} = -e(E_{\mathrm{red}} + 4.4)$ eV [28]. As can be seen in Table 1, the HOMO value for all copolymers is around −5.62 eV, and does not have obvious changes with different bipyridine contents. But the LUMO levels have big changes with introducing bipyridine unit into polymer main chain. For example, the LUMO level of PFN is around −2.14 eV, however, the LUMO level changes to −2.48 eV for PFN–Bpy10, which contains 10 mol% bipyridine units. The lower LUMO level after introducing bipyridine unit into copolymers is due to the electron-withdrawing property of bipyridine, which will lower the LUMO energy level.

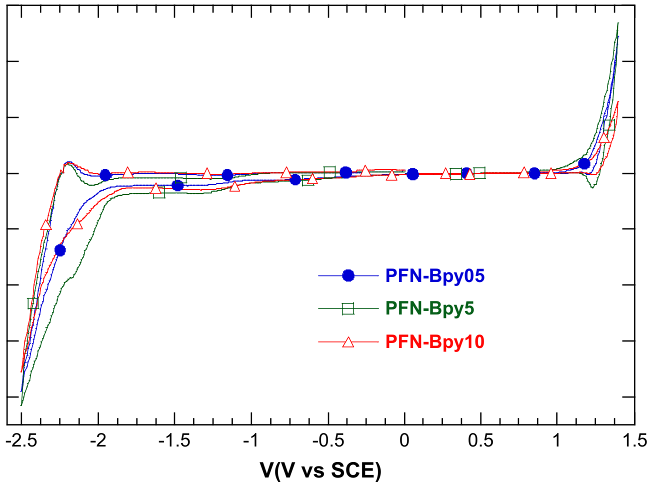

Fig. 4. Cyclic voltammograms (CVs) of the polymer films coated on platinum electrodes in 0.1 mol/L BuN_4PF_6, CH_3CN solution.

3.3. Electroluminescent properties

The electroluminescent properties of these copolymers were investigated. All copolymers were used as the emitting layer in a double-layer light-emitting device with configuration ITO/PEDOT/PVK/EML/Al (or Ba/Al). We note that the device efficiency was enhanced for all copolymers when PVK was used as the anode buffer layer [7]. The EL spectra are shown in Fig. 5. For PFN–Bpy copolymers, the EL spectra show a broad emission peaked at around 510 nm, which is similar with the EL spectra of PFN [7]. Significant broadening and enhancement at long wavelength shoulder in EL spectra in the thin film for varieties of polyfluorene or polyfluorene-based pyridine light-emitting polymers are common phenomena and investigated extensively [7]. The origin of line broadening and excimer formation has been widely investigated [29]. For rhenium copolymers, the EL spectra showed the emission from the rhenium complex peaked at around 645 nm, which indicated that the rhenium complex in polymer main chain could act as the narrow-band gap unit and the energy transfer from PFN to rhenium complex is very efficient.

3.4. The rhenium copolymers as electron injection layer

Charge injection and transport are the limiting factors for device efficiency and operating life-time. Most conjugated polymers are p-type semiconductors; balanced injection and transport in EL device are usually limited by the low electron affinity and low mobility of electron. In order to overcome the problem, the electron injection and/or transport layer usually is used in EL device. One of the principal demands for the polymer-based electron injection and/or transport layer in PLEDs is that the solvent used for spin-coating the electron injection and/or transport layer must not dissolve the underlying emissive polymers. As reported by our group [7–15], the aminoalkyl-polyfluorenes and their derivatives with aminoalkyl side chains can be used as electron injection and/or transport layer to improve the device performance. It will be interesting to check whether PFN–BpyRe can be used as an electron injection layer.

Here, we selected poly[2-(4-3′,7′-dimethyloctyloxy)-phenyl-*p*-phenylenevinylene] (P-PPV) and poly[9,9-dioctylfluorne-*co*-4,7-dithiophen-2-yl-2,1,3-benzothiadiazole] (PFO-DBT15) as emitting layers by inserting a very thin layer of PFN–Bpy5Re between EML and cathode to investigate the electron injection and/or transport properties. We note that device performance does not change with Re content in the copolymers.

Table 1
UV–vis absorption, electrochemical and photoluminescence properties of the copolymers (in solid films)

Copolymers	$\lambda_{\mathrm{abs\ max}}$ (nm)	E_{ox} (V)	E_{red} (V)	HOMO (eV)	LUMO (eV)	E_{gap} (eV)	$\lambda_{\mathrm{PLs\ max}}$ (nm)
PFN	390	1.21	−2.26	−5.61	−2.14	3.47	425
PFN–Bpy05	387	1.21	−2.17	−5.61	−2.23	3.38	421
PFN–Bpy5	384	1.22	−1.93	−5.62	−2.47	3.15	422
PFN–Bpy10	387	1.24	−1.92	−5.64	−2.48	3.16	420

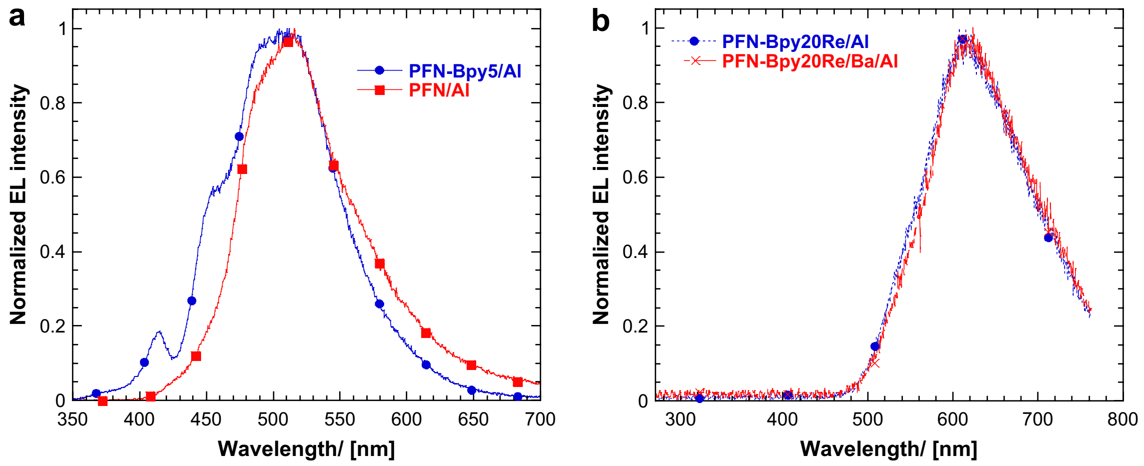

Fig. 5. The EL spectra of polymers (PFN–Bpy5 and PFN for comparison) (a) and rhenium copolymer (PFN–Bpy20Re) (b) at device structure of ITO/PEDOT:PSS/PVK/EML/Al.

Fig. 6 shows the current density–voltage (*J*–*V*) characteristic and light output from different device structures (three kinds of device structures: ITO/PEDOT/P-PPV/Ba/Al, ITO/PEDOT/P-PPV/PFN–Bpy5Re (7 nm)/Ba/Al and ITO/PEDOT/P-PPV/PFN–Bpy5Re (10 nm)/Ba/Al) while PPV as emission layer. Fig. 6 clearly shows that after inserting a thin layer of PFN–Bpy5Re between EML and Ba/Al, the device performances were significantly improved. In addition, the device performance with 7 nm of PFN–Bpy5Re layer is better than that with 10 nm of PFN–Bpy5Re layer (Fig. 6). Under the same current density, the devices with PFN–Bpy5Re layer have better brightness output and luminance efficiency than that with pure Ba/Al cathode. For example, at 10 mA/cm^2, the EQEs and luminance efficiency for devices with pure Ba/Al as cathode were 2.50% and 6.00 cd/A, respectively, with the luminance intensity of 609 cd/m^2 (Table 2). However, after inserting 7 nm of PFN–Bpy5Re layer, the corresponding EQEs and luminance efficiency reached 4.38% and 10.52 cd/A, respectively. It is important that the operating voltage was decreased after inserting a thin PFN–Bpy5Re layer (Table 2). Detailed device performance is given in Table 2. As shown in Fig. 7, while PFO-DBT as emission layer, the

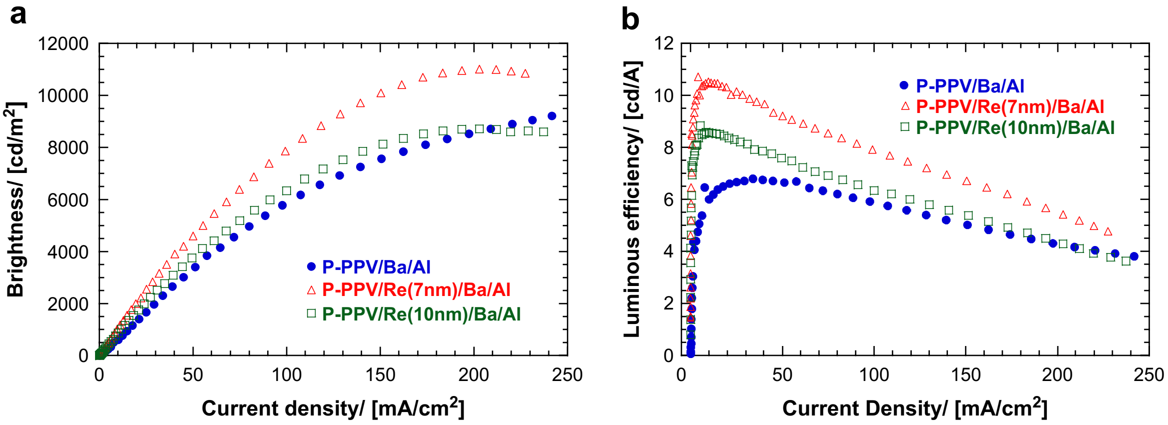

Fig. 6. The current density–brightness (a) and current density–luminance efficiency (b) curves of P-PPV devices with Ba/Al and PFN–Bpy5Re/Ba/Al as cathodes.

Table 2
The device performance of P-PPV devices with and without PFN–Bpy5Re as ETL layer

Device structures	At about 10 mA/cm^2						
	V_{th}[a] (V)	EQE[b] (%)	LE[c] (cd/A)	CE[d] (lm/W)	B[e] (cd/m^2)	Voltage (V)	Current density (mA/cm^2)
P-PPV/Re(7 nm)/Ba/Al	3.3	4.4	10.5	5.8	1015	5.7	9.7
P-PPV/Re(10 nm)/Ba/Al	3.4	3.6	8.6	4.8	869	5.6	10.2
PEDOT/P-PPV/Ba/Al	4.6	2.5	6.0	3.1	609	6.2	10.2

[a] Threshold voltage.
[b] External quantum efficiency.
[c] Luminous efficiency.
[d] Current efficiency.
[e] Brightness.

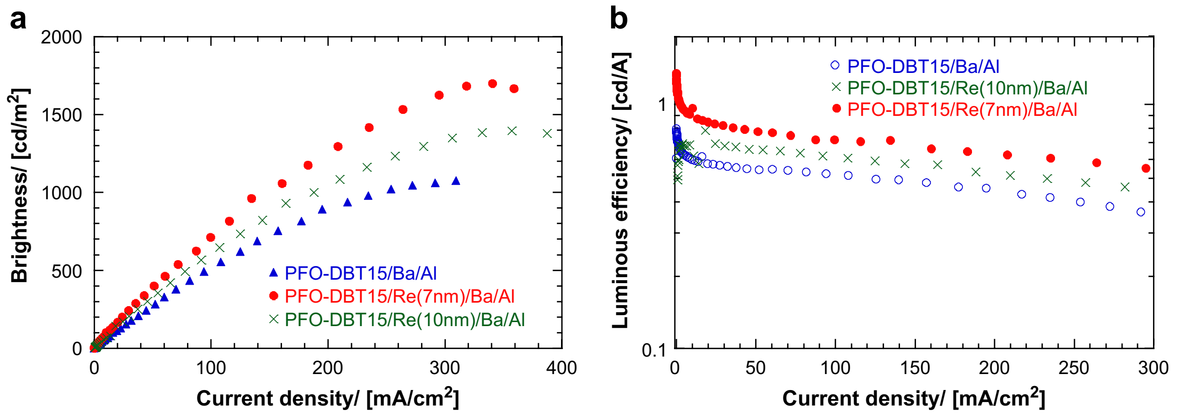

Fig. 7. The current density–brightness (a) and current density–luminance efficiency (b) curves of PFO-DBT15 devices with Ba/Al and PFN–Bpy5Re/Ba/Al as cathodes.

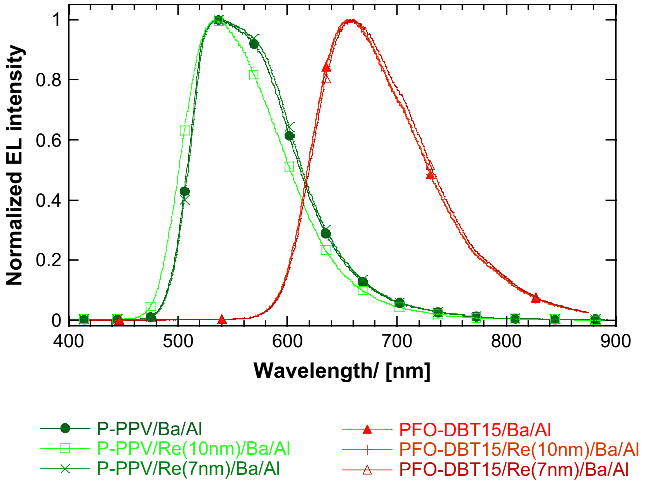

Fig. 8. The EL spectra of P-PPV and PFO-DBT15 devices with Ba/Al and PFN–Bpy5Re/Ba/Al as cathodes.

device performances can also improve after inserting a PFN–Bpy5Re thin layer. The maximum EQE, luminous efficiency and brightness output for device with structure of ITO/PEDOT/PFO-DBT15/PFN–Bpy5Re (10 nm)/Ba/Al were 1.42%, 0.8 cd/A and 1000 cd/m^2, respectively. However, after inserting 7 nm of PFN–Bpy5Re, the device performance was also significant improved and the corresponding maximum EQE, luminous efficiency and brightness output reached 2.39%, 1.34 cd/A and 1700 cd/m^2.

The EL spectra for the two types of cathodes (PFN–BpyRe/Ba/Al and Ba/Al) with P-PPV and PFO-DBT15 emission layers, respectively, as shown in Fig. 8 are almost identical. The results show that the recombination zone for the devices is located in the light-emitting layer (P-PPV and PFO-DBT15) and the PFN–BpyRe layer plays a role of the electron transport layer.

4. Conclusion

We have successfully synthesized a series of fluorene-based aminoalkyl-contained copolymers and their rhenium copolymers with different Bpy contents in main chain by the Suzuki cross-coupling reaction. The bipyridine-contained copolymers have good solubility in common organic solvents, such as toluene and chloroform. However, the rhenium copolymers, which were synthesized by coordinating with Re(CO)$_5$Cl, have different solubilities. The rhenium copolymers become insoluble in toluene and chloroform; instead have good solubility in polar solvents, such as methanol and DMF. The optoelectronic and electrochemical properties of these copolymers were studied. The electroluminescent properties of these copolymers were also investigated and we find that these rhenium copolymers can be used as the electron transport and/or injection layer in PLED. After inserting a thin rhenium copolymer layer between emission layer and cathode, a great improvement in EL performance could be achieved.

Acknowledgements

This work was supported by the Ministry of Science and Technology (MOST) of China, project number 2002CB613403 and NSFC project number 50433030.

References

[1] Burroughes JH, Bradley DDC, Brown AR, Marks RN, Mackay K, Friend RH, et al. Nature 1990;347:539.
[2] Sugura JL. Acta Polym 1998;49:319.
[3] Kraft A, Grimsdale AC, Holmes AB. Angew Chem Int Ed 1998;37:402.
[4] Kim DY, Cho HN, Kim CY. Prog Polym Sci 2000;25:1089.
[5] Bernius M, Inbasekaran M, O'Brien J, Wu W. Adv Mater 2000;12:1737.
[6] Akcelrud L. Prog Polym Sci 2003;28:875.
[7] Huang F, Wu HB, Wang DL, Yang W, Cao Y. Chem Mater 2004;16:708.
[8] Huang F, Hou LT, Wu HB, Wang XH, Shen HL, Cao W, et al. J Am Chem Soc 2004;126:9845.
[9] Huang F, Hou LT, Shen HL, Jiang JX, Wang F, Zhen HY, et al. J Mater Chem 2005;15:2499.
[10] Zhang Y, Xu YH, Niu QL, Peng JB, Yang W, Zhu XH, et al. J Mater Chem 2007;17:992.
[11] Zhang Y, Xiong Y, Sun YH, Zhu XH, Peng JB, Cao Y. Polymer 2007;48:3468.
[12] Zhang Y, Xiong Y, Liu RS, Peng JB, Cao Y. Acta Chim Sin 2007;65:2929.
[13] Wu HB, Huang F, Mo YQ, Yang W, Wang DL, Peng JB, et al. Adv Mater 2004;16:1826.

[14] Wu HB, Huang F, Peng JB, Cao Y. Org Electron 2005;6:118.

[15] Schanze KS, MacQueen DB, Perkins TA, Cabana LA. Coord Chem Rev 1994;94:993.

[16] Ley KD, Schanze KS. Coord Chem Rev 1998;287:171.

[17] Ley KD, Li Y, Johnson JV, Powell DH, Schanze KS. Chem Commun 1999:1749.

[18] Walters KA, Ley KD, Cavalaheiro CSP, Miller SE, Gosztola D, Wasielewski MR, et al. J Am Chem Soc 2001;123:8329.

[19] Ng PK, Gong X, Chan SH, Lam LSM, Chan WK. Chem—Eur J 2001;7:4358.

[20] Chan WK, Hui CS, Man KYK, Cheng KW, Wong HL, Zhu NY, et al. Coord Chem Rev 2005;249:1351.

[21] Walters KA, Dattelbaum DM, Ley KD, Schoonover JR, Meyer TJ, Schanze KS. Chem Commun 2001:1834.

[22] Zhang M, Lu P, Wang XM, He L, Xia H, Zhang W, et al. J Phys Chem B 2004;108:13185.

[23] Schwab PFH, Fleischer F, Michl J. J Org Chem 2002;67:443.

[24] Yang J, Jiang CY, Zhang Y, Yang RQ, Yang W, Hou Q, et al. Macromolecules 2004;37:1211.

[25] Yang RQ, Tian RY, Yan JA, Zhang Y, Yang J, Hou Q, et al. Macromolecules 2005;38:244.

[26] Zhang Y, Shi HH, Ke Y, Cao Y. J Lumin 2007;124:51.

[27] Liu B, Yu WL, Lai YH, Huang W. Macromolecules 2002;35:4975.

[28] Leuw DW, Simenon MMJ, Brown AR, Einerhand REF. Synth Met 1997;87:53.

[29] Yang W, Huang J, Liu CZ, Niu YH, Hou Q, Yang RQ, et al. Polymer 2004;45:865.